



RESEARCH ARTICLE

HORSESHOE KIDNEY: A PICTORIAL ESSAY FROM WOMB TO TOMB

*Neha Antil, Mahesh Kumar Mittal, Garvit Khatri and Mukul Sinha

Departments of Radiology & Imaging, Vardhman Mahavir Medical College and Safdarjang Hospital,
New Delhi – 110029, India

ARTICLE INFO

Article History:

Received 22nd July, 2017
Received in revised form
05th August, 2017
Accepted 29th September, 2017
Published online 17th October, 2017

Key words:

Horseshoe Kidney, Complications,
Multimodality Imaging.

ABSTRACT

The horseshoe kidney is the most frequent genitourinary anomaly, characterized by series of anatomical events of congenital fusion of both kidneys across midline, non-rotation, arrest of ascent and vascular changes. It is important to understand embryogenesis and development of HSK, which explains the vascular changes and related complications. Horseshoe kidney is more prone to a variety of complications, the common ones are pelvi-ureteric junction obstruction, infection, urolithiasis, trauma and malignancy. Multimodality imaging plays a vital role not just by providing information about the vascular supply to HSK but also helps in diagnosing associated complications in patients with HSK.

Copyright©2017, Neha Antil et al. This is an open access article distributed under the Creative Commons Attribution License, which permits unrestricted use, distribution, and reproduction in any medium, provided the original work is properly cited.

Citation: Neha Antil, 2017. "Horseshoe Kidney: A Pictorial Essay from Womb to Tomb." *International Journal of Current Research*, 9, (10), 58808-58814.

INTRODUCTION

The horseshoe kidney (HSK) is the most frequent fusion anomaly of the kidney, with an incidence of 0.25% of total population, which accounts 1 in 400 people, having male preponderance by 2:1 (Weizer *et al.*, 2003; Sharma *et al.*, 2015; O'Brien *et al.*, 2008; Natsis *et al.*, 2014; Jones *et al.*, 2009; Spinu *et al.*, 2015). It was first recognized at autopsy by DeCarpi in 1521 (Jones *et al.*, 2009; Spinu *et al.*, 2015). It is characterized by series of anatomical events of congenital fusion of both the kidneys across midline, ectopia, non-rotation and vascular changes (Sharma *et al.*, 2015; Natsis *et al.*, 2014). Congenital renal fusion occurs by parenchymal or fibrous isthmus commonly involving lower poles of both the kidneys or rarely may involve the upper poles. Ectopia results due to arrest of ascent of HSK, as the isthmus plugs under the origin of inferior mesenteric artery (IMA) from aorta, this results in variable blood supply from distal aorta and common iliac. Non-rotation occurs due to fusion and ectopia, which hinders normal renal rotation leading to anteriorly facing renal pelvis. Further, these events predispose HSK to various pathologies like pelvi-ureteric junction obstruction (PUJO), infection, urolithiasis, serious injuries following trauma and malignancies. HSK is at high risk of developing malignancies such as renal cell carcinoma, Transitional cell carcinoma, Wilm's tumour and carcinoid due to abnormal migration and proliferation of posterior nephrogenic cells that form a parenchymal isthmus (Natsis *et al.*, 2014).

Embryology

Normal kidneys develop in pelvis after union of ureteric bud with proliferated nephrogenic blastema, which occurs during fourth gestational week. Thereafter during 7th – 8th weeks it starts to ascend out of pelvis to reach its final position opposite the second lumbar vertebra and at the same time it undergoes a 90 degrees inward rotation along its long axis, so that the anteriorly facing renal pelvis turns medially (O'Brien *et al.*, 2008; Natsis *et al.*, 2014). (Figure 1) In contrary, HSK forms after fusion of lower poles of both kidneys that lies in close proximity in the pelvis. The fusion is thought to occur due to abnormal flexion or growth of the developing spine and other pelvic organs that causes fusion of nephrogenic blastemas of non-encapsulated immature kidneys. After fusion, it ascends up to the junction of aorta with IMA to lie at the level of lower lumbar vertebra, anterior to aorta and IVC as isthmus hooks at this level and cannot ascend further (O'Brien *et al.*, 2008; Natsis *et al.*, 2014). (Figure 2)

Anatomy of HSK

Horseshoe kidney can be classified by its shape into two types, U-shaped HSK and L-shaped HSK. U-shaped HSK is formed after the medial fusion of both kidneys placed symmetrically on either side of vertebra and L-shaped HSK is formed as a result of lateral fusion between a horizontal part of one kidney with the vertical part of other kidney and the isthmus lies lateral to the midline (Natsis *et al.*, 2014). Based on the position and features of isthmus Matsumoto *et al.*, 2015 classified HSK into Type Aa fusion of superior poles, Type Ab fusion of inferior poles (most common), Type Ba fusion by

*Corresponding author: Neha Antil
VMMC and Safdarjung Hospital, India.

fibrous tissue, Type Bb parenchymal fusion directly and Type Bcfusion by mediators.

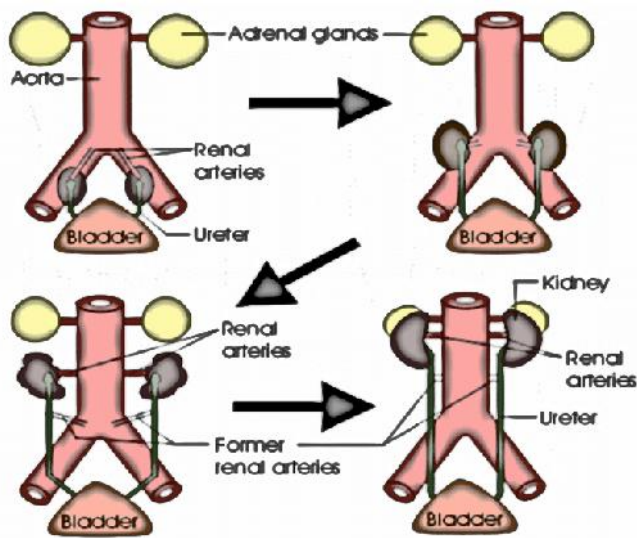


Figure 1. Schematic diagram showing normal embryogenesis of kidneys. During 4th gestational week, normal kidneys start to develop which is followed up ascent and 90degrees inward rotation to finally lie at the level of L2 vertebra at around 7th-8th week of gestation

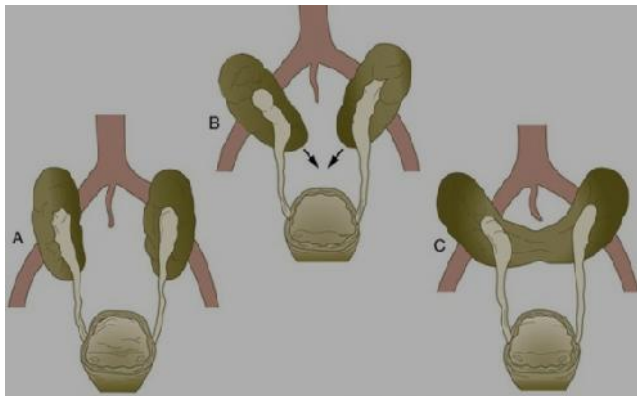


Figure 2. Schematic diagram showing embryogenesis of horseshoe kidney. (A,B) shows fusion of the lower poles of both the kidneys in the pelvis, (C) shows arrest of ascent of the fused kidneys at the level of inferior mesenteric artery

Vascular anatomy

Horseshoe kidney has a variable arterial supply, it consists of one renal artery to each kidney in around 30% of cases but can have two or three renal arteries supplying one or both the kidneys (Türkvtan *et al.*, 2009; Kikkawa *et al.*, 2015). The isthmus and parenchymal masses may receive supply from main renal artery or from aorta, inferior mesenteric, common iliac or internal iliac arteries, depending on the level of ascent of HSK in abdomen (Sharma *et al.*, 2015; Türkvtan *et al.*, 2009). This has a significant clinical significance, it is important to know blood supply before operating a HSK with multiple renal arteries, to avoid hazardous complication and viability of the organ. It has been proposed to completely remove HSK with large portion of abdominal aorta and IVC so as to preserve multiple renal vessels to maintain the vitality of the allograft in cases of transplant surgery and to achieve adequate hemostasis (Natsis *et al.*, 2014). Graves classified

arterial supply of HSK in six patterns, (Sharma *et al.*, 2015; Natsis *et al.*, 2014) (Figure 3)

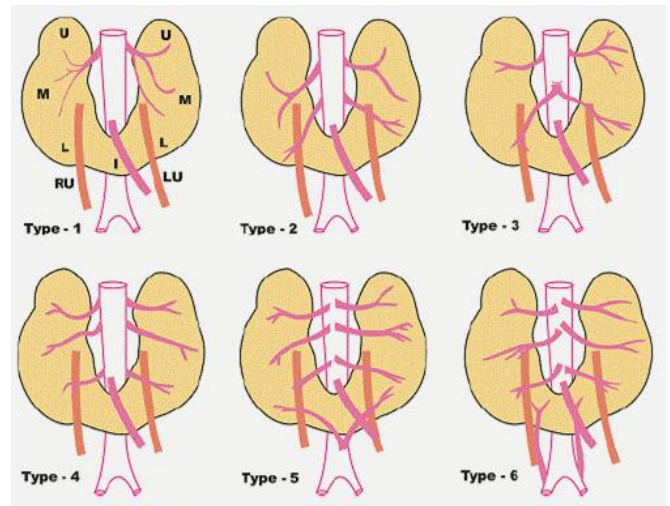


Figure 3. Schematic diagram showing vascular anatomy of horseshoe kidney, classified by Graves into six patterns (Type 1-6)

- Type 1:** A single artery, excluding the collateral circulation, supplies every HSK segment; upper (U), middle (M), lower (L).
- Type 2:** Upper and middle segments of each kidney supplied by a single artery, with a vessel from aorta entering each lower segment.
- Type 3:** Upper and middle segments of each kidney supplied by a single artery, with arteries to the lower segment arising from aorta by common trunk.
- Type 4:** All three segments are supplied by separate arteries, arising from aorta.
- Type 5:** All three segments are supplied by separate arteries, arising from aorta. Fused isthmus supplied by arteries, which arise above or below the isthmus. These can be unilateral or bilateral and originate from the aorta independently or by common trunk.
- Type 6:** Fused isthmus supplied by arteries originating from common iliac or internal iliac or median sacral artery.

Imaging of horseshoe kidney

HSK is usually an incidental finding which is commonly seen while performing multiple imaging studies like ultrasound (USG) abdomen, intravenous urography (IVU), multidetector computed tomography (MDCT), magnetic resonance imaging (MRI) and scintigraphy (O'Brien *et al.*, 2008; Natsis *et al.*, 2014). It can occasionally be picked on plain radiographs if observed sharp-eyed. Renal outline is well delineated on plain radiographs as it is surrounded by perinephric fat. HSK have altered renal axis with lower poles being more close to the spine in the midline, just reverse of normal kidney and have lower position as compared to normal kidneys. Plain radiographs also have value in identifying renal and ureteric calculi (O'Brien *et al.*, 2008) (Figure 4). IVU is usually a first line of investigation, followed by CT scanning and scintigraphy in doubtful cases (Moloney *et al.*, 2014). On IVU, HSK appears either U or L-shaped structure depending on the amount of tissue on each side of spine. The lower pole calyces are rotated medially near isthmus, facing vertebrae and lie medial to ureters, giving appearance of 'hand holding calyces'. The ureters when it crosses down the isthmus, it first curves laterally then assumes a normal medial course resulting in

'flower vase appearance'. (Figure 5) Renal pelvises are usually extrarenal in location, directed anteriorly and appear enlarged. This normal appearance of large extrarenal pelvis can be differentiated from Pelvi-ureteric junction obstruction by administering diuretics before performing IVU. In PUJ Obstruction, there will further more dilatation of renal pelvis with abrupt narrowing at PUJ and delayed clearance of contrast. HSK is more prone to urinary stasis and reflux leading to hydronephrosis, which can be well demonstrated on IVU.



Figure 4. 40year old female patient with an already diagnosed horseshoe kidney, Plain radiograph reveals two radioopaque densities in the pelvis, which were confirmed as bilateral vesicoureteric calculus on ultrasound. Note is made of the abnormal renal axis with lower pole of both kidneys lying close to the spine



Figure 5. 39 year old female patient presented with right flank pain, Intravenous urography in pyelographic phase reveals features diagnostic of a HSK. The lower pole calyces of both kidneys are rotated medially lying medial to ureters like 'hand holding calyces' and both ureter are laterally placed in proximal extent then coursing medially forming a 'flower vase appearance'

The limitation of IVU is it cannot distinguish fibrous versus parenchymal isthmus, which can be dealt with that of CT or scintigraphy. Technetium (^{99}Tc) bone scan imaging shows increase uptake by the functioning renal tissue and parenchymal isthmus forming a continuous band across midline, thus distinguish between fibrous and parenchyma isthmus (O'Brien *et al.*, 2008). While ^{99}Tc -Dimercaptosuccinic acid nuclear scan is used to evaluate renal

scarring in children (O'Brien *et al.*, 2008). Ultrasound abdomen shows curved configuration of HSK with poor visualization of lower poles, when scanned in the renal fossa. The two lower poles of kidney are seen to fused by an isthmus which is seen to lie in the paraspinal location anterior to aorta and IVC (O'Brien *et al.*, 2008). It is easy to make diagnosis in children and thin patients but is difficult to pick in obese patients. MDCT urography is a comprehensive 'one-stop' investigation for imaging upper and lower urinary tract (Türkvatan *et al.*, 2009; Lawler *et al.*, 2005; Maher *et al.*, 2004). Triple phase MDCT urography is performed at most of institutes for evaluation of patients with renal pathologies. It comprises of three phases: unenhanced, nephrographic phase and pyelographic phase.

However to reduce radiation dose to patient some institute uses dual energy CT or split bolus CT urography. The patient is positioned supine and an initial unenhanced scans are obtained from bilateral domes of diaphragm to the pubic symphysis, this is to detect urinary tract calculi. Second phase is nephrographic phase obtained for renal parenchymal evaluation, which is acquired following intravenous iodinated contrast administration, after a delay of 90-100sec. Enhancing functional isthmus of HSK can be differentiated from non-enhancing fibrous isthmus on this phase. This is followed by pyelographic phase taken 5-10mins after contrast administration to evaluate pelvicalyceal system, ureters and urinary bladder. Sometime, a delayed pyelographic is also obtained after 45-60mins delay in cases of delayed excretion of contrast. For evaluation of HSK, additional scan is performed in arterial phase approximately 30sec after the contrast administration, used to evaluate blood supply to HSK. Multiple post CT processing tools like Multiplanar reformation (MPR), MIP (maximum intensity projection), 3D Volume rendered technique (VRT) can be obtained, which provides additional information by generating angiograms (Figure 6 and 7), Urograms and 3D perspective for planning surgery. Thus MDCT urography is the modality of choice for the assessment of HSK, as it distinguishes functional parenchymal isthmus versus fibrous isthmus, allows precise information of the anatomy and helps in evaluating the potential complications associated with HS. MRI has no added advantage over CT in diagnosing HSK and its complications. However protects from hazardous ionizing radiation from that of CT (O'Brien *et al.*, 2008).

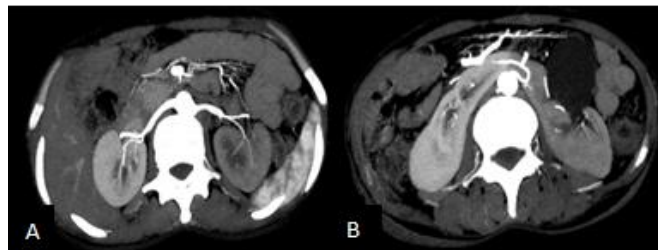


Figure 6. 25 year old female patient with HSK, Axial CT images (a,b) in angiographic phase show single renal artery supplying both the kidneys (a), with an additional separate branch supplying isthmus originating from aorta independently (b). Note is made of left sided extrarenal pelvis

Complications of horseshoe kidneys

About one-third of patients remain asymptomatic and discovered incidentally (O'Brien *et al.*, 2008). Rest becomes symptomatic secondary to the occurrence of complications in

HSK. These complications develop due of complex embryogenesis and anatomy of HSK then normal kidney. The variable blood supply, presence of midline isthmus, abnormal insertion and course of ureter contributes to the development of renal complications, resulting secondary to obstruction, stone formation, stasis and urinary tract infection (Sharma *et al.*, 2015; O'Brien *et al.*, 2008; Natsis *et al.*, 2014; Naveena and Mrudula, 2017; Castro and Green, 1975; Je *et al.*, 2015). Imaging plays a pivotal role in evaluation of these complications, and MDCT is the modality of choice.



Figure 7. 28 year male patient of HSK, Coronal CT image in angiographic phase shows single artery supplying the right kidney and two renal arteries are seen supplying the left kidney

Pelviuretericjunction obstruction

PUJO is the most common observation and cause of hydronephrosis in HSK patients, accounting for 14-35% of cases. It is usually unilateral but may be seen bilaterally (O'Brien *et al.*, 2008; Panda *et al.*, 2014; Singhania *et al.*, 2015). The factors contributing to obstruction are high insertion of ureter into the renal pelvis, crossing vessels and narrowing at pelvi-ureteric junction. The renal pelvis and ureter in HSK are anteriorly placed with high ureteric insertion into renal pelvis with further ureters lie anterior to isthmus leads to a kink, resulting in obstruction and hydronephrosis (O'Brien *et al.*, 2008; Natsis *et al.*, 2014; Panda *et al.*, 2014; Singh *et al.*, 2013). The diagnosis can be made on IVU with a typical appearance of ballooned out large, anteriorly placed renal pelvis and narrowing at pelvi-ureteric junction. (Figure 8) To differentiate normally enlarged renal pelvis from PUJO, a diuresis radioisotope renal scan or IVU can be performed. In cases of PUJO there will further distension of renal pelvis with delayed clearance of isotope. Role of ultrasound and CT is to assess degree of hydronephrosis, cortical thickness and vascular supply, before treating a PUJO (O'Brien *et al.*, 2008) (Figure 9).

Urolithiasis

Urolithiasis is a main complication of HSK with a prevalence of 20-60% of all cases, which is often associated with PUJO.^[3,16] The impaired drainage through mal-oriented renal

calyces, high position of pelvi-ureteric junction, PUJO and reflux are contributing factors resulting in stone formation secondary to stasis and infection (O'Brien *et al.*, 2008; Natsis *et al.*, 2014; Stasinou *et al.*, 2017). Multiple calculi or large staghorn calculi are formed, which can be seen on plain radiographs (Figure 10) or on ultrasound. IVU allows the precise localization of renal calculi and evaluation of grade of hydronephrosis. CT urography is more sensitive in detection and localization of calculus in doubtful cases.



Figure 8. 29year old male presented with right flank pain, Intravenous urography in pyelographic phase reveals a HSK showing dilatation of right renal pelvis with abrupt tapering at pelvi-ureteric junction and proximal hydronephrosis, diagnostic of PUJO Obstruction

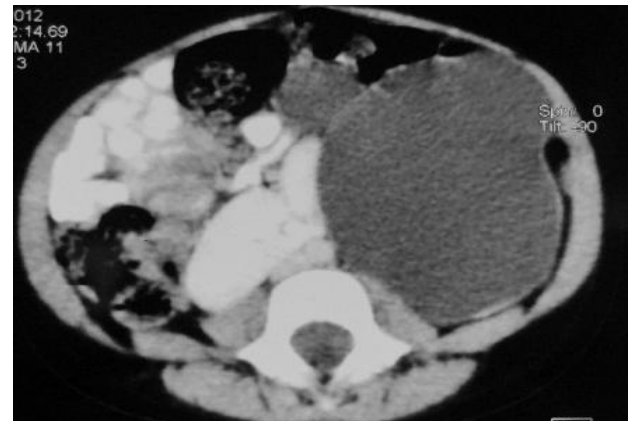


Figure 9. 8 year old male patient of HSK presented with left flank pain, axial post contrast CT image shows gross dilatation of pelvicalyceal system with abrupt tapering at PUJ with cortical thinning, suggesting PUJO in HSK

Trauma

HSK are more prone to renal injuries related to blunt abdominal trauma due to its low position in abdomen and presence of midline isthmus, which results in compression of HSK against lumbar vertebral spine (O'Brien *et al.*, 2008; Natsis *et al.*, 2014). CT is the modality of choice to assess function and the grade of renal injury, thus help in planning appropriate treatment (Figure 11).



Figure 10. A 32 year old male patient with HSK, Plain radiograph shows bilateral staghorn calculi with few secondary calculi in both kidneys

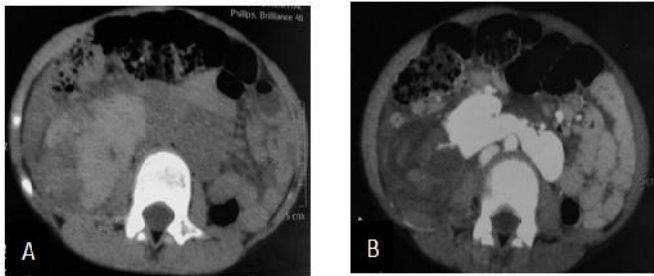


Figure 11. 29 year old male patient presented with blunt abdominal trauma, Non contrast axial CT scan image (a) reveals an area of hyperdensity within right renal parenchyma and in posterior perinephric space suggestive of hemorrhage. Post contrast axial CT scan image reveals (b) a non-enhancing hypodense area predominantly involving lower pole of right kidney suggestive of renal laceration, contusion and infarction in a HSK

Tumours

The first case of malignant tumour in a HSK was diagnosed in 1895 (Castro and Green, 1975). The tumour pathology is rare in HSK, however the tumour incidence is 3-4 times higher the normal kidney (Spinu *et al.*, 2015; Alamer, 2013). It can occur de novo or secondary to complications like urinary stasis. HSK are associated with variety of benign and malignant tumours (O'Brien *et al.*, 2008). Most common malignant tumour associated with HSK is renal cell carcinoma, which accounts for 45% of all tumours (O'Brien *et al.*, 2008; Jones *et al.*, 2009; Spinu *et al.*, 2015; Alamer, 2013). It is being proposed that HSK can result in a teratogenic event, as it involves abnormal migration and proliferation of posterior nephrogenic cells that forms a parenchymal isthmus (O'Brien *et al.*, 2008; Natsis *et al.*, 2014). Thus isthmus is the most common site for development of tumours (O'Brien *et al.*, 2008). Transitional cell carcinoma accounts for 20% of tumours with threefold

increased incidence in patients with HSK, possibly related to prolonged exposure to urinary stasis, infections and calculi (O'Brien *et al.*, 2008; Jones *et al.*, 2009). Carcinoid and Wilmstumours are also associated with HSK with Wilmstumour accounting for 28% of malignant lesions with doubling risk in HSK. However renal carcinoids are relatively rare and are believed to originate from neuroendocrine cells present within teratomatous tissue of HSK (Natsis *et al.*, 2014). Among benign tumours, Oncocytomas are most frequent benign tumour associated with HSK (O'Brien *et al.*, 2008). Imaging (Computed tomography and magnetic resonance imaging) plays a vital role in identification of these renal tumours and their staging. (Figure 12) Additionally it can assess renal vascular anatomy and anatomical variations, in order to avoid hazardous intraoperative complications. Thus a vascular map using CT angiography must be attained before planning a surgery.

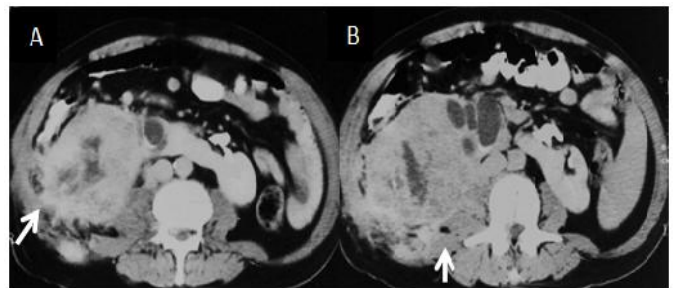


Figure 12. 55 year old male patient with a HSK, Axial post contrast CT scan images (a,b) of HSK shows a heterogeneously enhancing soft tissue mass lesion with areas of central necrosis seen arising from right kidney and involving part of isthmus. Also there is focal infiltration of the mass lesion in the surrounding right lateral abdominal wall muscles (a) and right psoas muscle (b). (shown by white arrow) HPE confirmed the diagnosis of renal cell carcinoma

Miscellaneous



Figure 13. 42 year old female presented with right hypochondrium pain, Axial post contrast CT scans (a,b) reveals presence of a HSK with mass in the gallbladder fossa, liver metastasis and retroperitoneal metastatic nodes. Sagittal CT scan in bony window (c) shows a congenital block vertebra involving C4-5 vertebrae

HSK is also associated with multiple congenital anomalies, which includes chromosomal, skeletal, neurological and gastrointestinal abnormalities, occurring in about 85% of patients (Sharma *et al.*, 2015; O'Brien *et al.*, 2008; Natsis *et al.*, 2014; Je *et al.*, 2015). Numerous chromosomal abnormalities are seen to co-exist with HSK which are Turner syndromes (60%), Down and Edwards syndromes (20%). Patau and Gardner syndromes are also seen to co-exist with HSK. Skeletal abnormalities such as congenital block vertebra (Figure 13), hemivertebra kyphosis, scoliosis and macrognathia, neurological abnormalities such as

encephalocele, meningomyelocele and spina bifida and gastrointestinal abnormalities such as supernumerary kidneys, ureterocele (Ameli *et al.*, 2015) undescended testis, Bicornuate/septate vagina and hypospadias are seen to co-exist with HSK. HSK are also seen to be associated with few extrarenal tumors like neuroblastoma, teratoma (Figure 14), Hodgkin lymphoma and round cell tumors (osteosarcoma/Ewing's sarcoma) (Figure 15) as reported by Je *et al.* A vigilant investigation must be performed to rule out these associated anomalies.

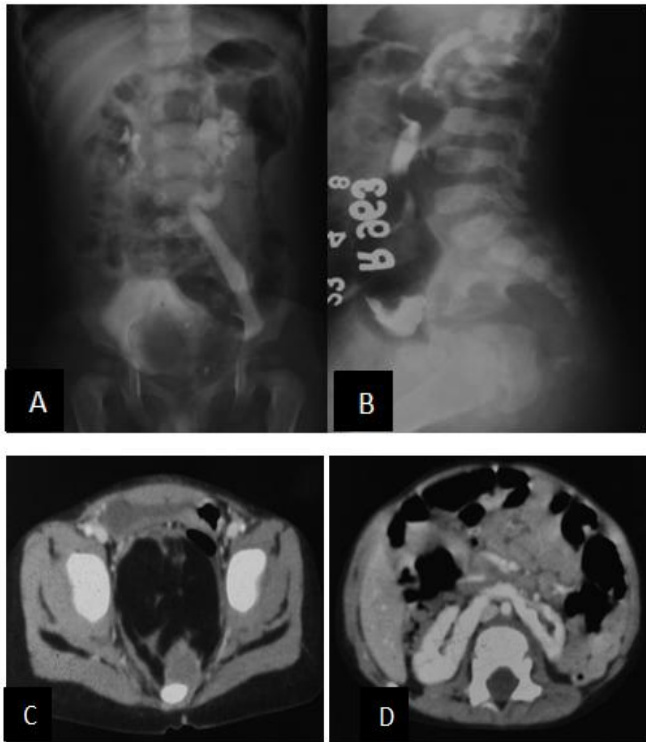


Figure 14. 4 year old male patient complained of abdominal distention and difficulty in passing stools, IVU films in excretory phase (a,b) show left sided hydronephrosis and increased pre sacral space with anterolateral displacement of UB. Axial post contrast CT scan images (c,d) of the same patient, reveal large fat and soft tissue containing mass lesion arising from sacrococcygeal region, extending to the presacral space (c). A diagnosis of sacrococcygeal teratoma was made, which was confirmed on histopathology with incidental note of a HSK (d)

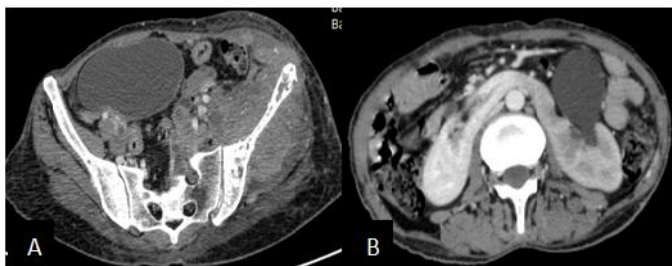


Figure 15. 25year old male patient presented with soft tissue swelling around left hip joint, Axial post contrast CT scans show (a) malignant tumour involving left iliac blade, which was a histopathological proven round cell tumour co-existent with HSK (b) and note is made of left sided hydronephrosis

Conclusion

HSK is by far the most common congenital fusion anomaly of genitourinary system. All HSKs must be carefully investigated

to assess renal vascular anatomy as it has a variable blood supply from aorta. Thus vascular maps must be attained using MDCT angiography before operating a HSK, to avoid hazardous complication and viability of the organ. Imaging thus plays an important role for the treating surgeons by providing useful information about the vascular supply and collecting system. It also helps in evaluating pathologies like PUJ obstruction, infection, urolithiasis, trauma and malignancies in patients with HSK, perhaps helps in early intervention to avoid organ failure.

REFERENCES

- Alamer A. 2013. Renal cell carcinoma in a horseshoe kidney: radiology and pathology correlation. *J Clin Imaging Sci.*, 3:12.
- Ameli M, Jarhi A, Mahmoudabadi A. 2015. Bilateral Ureterocele Along With Horseshoe Kidney in an Adult: A Case Report and Review of Literature. *Thrita.*, 4:33549.
- Castro JE, Green NA. 1975. Complications of horseshoe kidney. *Urology*, 6:344-7.
- Je BK, Kim HK, Horn PS. 2015. Incidence and spectrum of renal complications and extrarenal diseases and syndromes in 380 children and young adults with horseshoe kidney. *American Journal of Roentgenology*, 205:1306-14.
- Jones L, Reeves M, Wingo S, Babanoury A. 2009. Malignant tumor in a horseshoe kidney. *Urology Journal*, 4:46-8.
- Kikkawa K, Wakamiya T, Kusumoto H, Matsumura N, Kohjimoto Y, Hara I. 2015. Transplantation of Horseshoe Kidney from Living, Genetically Unrelated Donor. Case reports in transplantation, 1-4.
- Lawler LP, Jarret TW, Corl FM, Fishman EK. 2005. Adult Ureteropelvic Junction Obstruction: Insights with Three-dimensional Multi-Detector Row CT 1. *Radiographics*, 25:121-34.
- Maher MM, Kalra MK, Rizzo S, Mueller PR, Saini S. 2004. Multidetector CT urography in imaging of the urinary tract in patients with hematuria. *Korean journal of radiology*, 5:1-10.
- Moloney F, Murphy KP, Twomey M, O'Connor OJ, Maher MM. 2014. Haematuria: an imaging guide. *Advances in urology*, 17.
- Natsis K, Piagkou M, Skotsimara A, Protogerou V, Tsitouridis I, Skandalakis P. 2014. Horseshoe kidney: a review of anatomy and pathology. *Surgical and Radiologic Anatomy*, 36:517-26.
- Naveena S, Mrudula C. 2017. Horseshoe kidney: a case report. *International Journal of Research in Medical Sciences*, 1:304-7.
- O'Brien J, Buckley O, Doody O, Ward E, Persaud T, Torreggiani W. 2008. Imaging of horseshoe kidneys and their complications. *Journal of medical imaging and radiation oncology*, 52:216-26.
- Panda SS, Bajpai M, Jana M, Baidya DK, Kumar R. 2014. Anderson-Hynes pyeloplasty with isthmotomy and lateropexy in horseshoe kidneys with pelviureteric junction obstruction in children. *Indian J Urol.*, 30:161-163.
- Sharma V, Ramesh Babu C.S, Gupta O.P. 2015. Horseshoe Kidney: A Multidetector Computed Tomography Study. *Int J Anat Res.*, 3:1049-1055.
- Singh A, Bajpai M, Sharma SP. 2013. Horseshoe kidney with right moiety pelviureteric junction obstruction. *Journal of progress in paediatric urology*, 16:20.
- Singhania PP, Raut NR, Shringarpure SS, Tiwari N, Sathe S. 2015. Horseshoe Kidney with Bilateral Ureteropelvic

- Junction Obstruction with Multiple Renal Calculi: A Case Report. *Int J Sci Stud.*,3:233-235.
- Spinu D, Aungurenci A, Marcu D, M dan V, Bratu O, Mischianu D. 2015. Neoplasia in horseshoe kidney-A case report. *RevistaRomân de Urologie nr*, 14:70.
- Stasinou T, Bourdounis A, Masood J. Forming a stone in pelviureteric junction obstruction: Cause or effect? *International Braz J Urol.*, 43:13-19.
- Türkvatan A, Ölçer T, Cumhuri T. 2009. Multidetector CT urography of renal fusion anomalies. *Diagnostic and Interventional Radiology*, 15:127.
- Weizer AZ, Silverstein AD, Auge BK, Delvecchio FC, Raj G, et al. 2003. Determining the incidence of horseshoe kidney from radiographic data at a single institution. *The Journal of urology*, 170:1722-6.
